



Contents lists available at SciVerse ScienceDirect

Spectrochimica Acta Part A: Molecular and Biomolecular Spectroscopy

journal homepage: www.elsevier.com/locate/saa

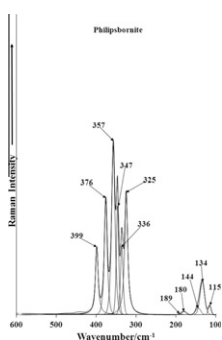
A vibrational spectroscopic study of philipsbornite $\text{PbAl}_3(\text{AsO}_4)_2(\text{OH})_5 \cdot \text{H}_2\text{O}$ -molecular structural implications and relationship to the crandallite subgroup arsenates

Ray L. Frost^{a,*}, Yunfei Xi^a, Ross E. Pogson^{a,b}, Ricardo Scholz^{a,c}^a Chemistry Discipline, Faculty of Science and Technology, Queensland University of Technology, GPO Box 2434, Brisbane Queensland 4001, Australia^b Geosciences (Mineralogy & Petrology), The Australian Museum, 6 College St., Sydney NSW 2010, Australia^c Geology Department, School of Mines, Federal University of Ouro Preto, Campus Morro do Cruzeiro, Ouro Preto, MG 35,400-00, Brazil

HIGHLIGHTS

- ▶ The presence of arsenic in the environment is a hazard.
- ▶ The accumulation of arsenate in the formation of minerals provides a mechanism for the remediation of arsenate contamination.
- ▶ The formation of the crandallite group provides a mechanism for arsenate accumulation.
- ▶ Raman spectroscopy complimented with infrared spectroscopy has enabled philipsbornite to be studied.

GRAPHICAL ABSTRACT



ARTICLE INFO

Article history:

Received 1 August 2012

Accepted 31 October 2012

Available online 22 November 2012

Keywords:

Philipsbornite

Arsenate

Arsenic remediation

Crandallite

Molecular structure

ABSTRACT

The presence of arsenic in the environment is a hazard. The accumulation of arsenate by a range of cations in the formation of minerals provides a mechanism for the remediation of arsenate contamination. The formation of the crandallite group of minerals provides a mechanism for arsenate accumulation. Among the crandallite minerals are philipsbornite, arsenocrandallite and arsenogoyazite. Raman spectroscopy complimented with infrared spectroscopy has enabled aspects of the structure of philipsbornite to be studied.

The Raman spectrum of philipsbornite displays an intense band at around 840 cm^{-1} attributed to the overlap of the symmetric and antisymmetric stretching modes. Raman bands observed at 325, 336, 347, 357, 376 and 399 cm^{-1} are assigned to the $\nu_2(\text{AsO}_4)^{3-}$ symmetric bending vibration (E) and to the ν_4 bending vibration (F_2). The observation of multiple bending modes supports the concept of a reduction in symmetry of the arsenate anion in philipsbornite. Evidence for phosphate in the mineral is provided. By using an empirical formula, hydrogen bond distances for the OH units in philipsbornite of 2.8648 Å, 2.7864 Å, 2.6896 Å and 2.6220 cm^{-1} were calculated.

© 2012 Elsevier B.V. All rights reserved.

Introduction

The mineral philipsbornite $\text{PbAl}_3(\text{AsO}_4)_2(\text{OH})_5 \cdot \text{H}_2\text{O}$ [1] is a member of the crandallite subgroup [2,3] of the alunite supergroup. It is the lead analogue of arsenocrandallite $(\text{Ca,Sr})\text{Al}_3(\text{AsO}_4)_2(\text{OH})_5$.

H_2O and arsenogoyazite $(\text{Sr,Ca,Ba})\text{Al}_3(\text{AsO}_4)_2(\text{OH,F})_5 \cdot \text{H}_2\text{O}$, and the arsenate analogue of plumbogummite $\text{PbAl}_3(\text{PO}_4)_2(\text{OH})_5 \cdot \text{H}_2\text{O}$. Philipsbornite forms a continuous series of solid solutions with these minerals [4]. The philipsbornite–segnetite series is well known. Philipsbornite is known from a number of locations worldwide [1,5–8]. In Australia, philipsbornite can be sourced from the Kintore open cut mine, New South Wales, Anticline Deposit, Ashburton Downs Station, Western Australia and of course from

* Corresponding author. Tel.: +61 7 3138 2407; fax: +61 7 3138 1804.

E-mail address: r.frost@qut.edu.au (R.L. Frost).

Red Lead Mine, Tasmania, Australia [9]. Arsenate and phosphate minerals including philipsbornite are found in Australian soils [10]. The mineral is hexagonal with point group: $3\ 2/m$. The cell data is Space Group: $R3m$, $a = 7.11\text{--}7.17$, $c = 17.05\text{--}17.18$, and $Z = 3$. Philipsbornite is a rare secondary mineral in the oxidised zone of hydrothermal polymetallic mineral deposits and is associated with crocoite, hidalgoite, gorceixite. The stability of many lead arsenate minerals have been reviewed [11].

The reason for this research is that minerals such as philipsbornite are found in soils and in old mine sites. Therefore, this research focuses on the spectroscopic determination of philipsbornite and consequential molecular structure. Raman spectroscopy has proven very useful for the study of minerals [12–19]. Indeed, Raman spectroscopy has proven most useful for the study of diagenetically related minerals as often occurs with minerals containing arsenate and sulphate groups, including philipsbornite and crandallite. Raman spectroscopy is especially useful when the minerals are X-ray non-diffracting or poorly diffracting and very useful for the study of amorphous and colloidal minerals [20–29]. Philipsbornite is a mineral which falls into this category.

Due to the somewhat amorphous nature of philipsbornite, the application of vibrational spectroscopy is very important. Only through vibrational spectroscopy can any concepts of the molecular structure of the mineral philipsbornite be determined. The minerals act as a sink for both phosphate and arsenate waste mine dumps. Further the minerals have been found in old or ancient burial sites. Some vibrational spectroscopic studies of the related arsenate containing minerals have been undertaken [30]. Some assignment of bands was undertaken and the spectra were simply reported without any explanation [30]. There is a vital need to study the molecular structure of these types of minerals in more detail.

The first study concerning the spectroscopic characterisation of arsenate bearing minerals of the crandallite group was reported by Gevorkyan et al. [31]. In recent years, the spectroscopic study of arsenates of the crandallite subgroup was improved by different studies, with special emphasis to the minerals segnitite [32], dussertite [33] and arsenogorceixite [34]. To the best of our knowledge, there have no published papers on the Raman spectroscopy of philipsbornite. Raman spectroscopy has proven very useful for the study of minerals. Indeed, Raman spectroscopy has proven most useful for the study of diagenetically related minerals as often occurs with minerals containing phosphate and arsenate groups. This paper is a part of systematic studies of vibrational spectra of the arsenates related to the crandallite subgroup. The objective of this research is to report the Raman spectra of philipsbornite, to relate the spectra to the molecular structure of the mineral and to compare the philipsbornite spectra with other crandallite minerals.

Experimental

Mineral

The philipsbornite mineral sample was loaned from The Australian Museum and is registered sample number D 45432. The mineral originated from the Red Lead mine [35]. The Red Lead Mine is located on the southern edge of the Dundas mining district. The Red Lead ore body is likely connected to the Adelaide Mine that is located on the northern side of the Dundas Ultramafic Complex.

The Dundas Ultramafic Sequence consists of a sequence of volcanic and sedimentary rocks of Eocambrian–Cambrian age. The sequence was formed in elongate rift troughs within and between regions of polydeformed Precambrian siltstone, orthoquartzite, and minor volcanic rocks. The stratigraphic sequence is represented by sediments of the Success Creek Group which unconformably overlie the Precambrian basement. This sequence is conformably

overlain by the Crimson Creek Formation, that consists of basic volcanoclastic sedimentary rocks with tholeiitic lavas [36].

Following the Crimson Creek Formation, a phase of high magnesium andesitic volcanism extruded. During the early Middle Cambrian a third phase of volcanic activity starts and have produced low-titanium tholeiitic lavas which interdigitate with basal conglomerate of the Dundas Group. In the late Middle Cambrian a subaerial acid to intermediate volcanic phase, the Mt. Read volcanics, formed contemporaneously with the sedimentary rock sequences of the Dundas Group. During Late Cambrian to Early Devonian, the southeastern part of the Dundas Trough and most of the Mt. Read volcanic belt were covered by marine sediments (Owen Conglomerate, Gordon Limestone and the Eldon Group) [36].

The surface gossans at the Red Lead Mine lie on the contact of the serpentinites with the Dundas series rocks. The mines originally all worked silver and lead-rich sulphide and carbonate primary ores, but were mostly developed in deeply weathered, to goethite-rich vuggy gossans. These gossanous zones contain a variety of unusual chrome and lead-bearing secondary minerals including crocoite (PbCrO_4), grimaldiite ($\text{CrO}(\text{OH})$), petterdite ($\text{PbCr}_2(\text{CO}_3)_2(\text{OH})_4\cdot\text{H}_2\text{O}$), a Cr–Mn oxide, Cr-rich mimetite ($\text{Pb}_5(\text{AsO}_4)_3\text{Cl}$) and Cr-rich philipsbornite ($\text{PbAl}_3(\text{AsO}_4)(\text{AsO}_3\text{OH})(\text{OH})_6$).

Raman spectroscopy

Crystals of philipsbornite were placed on a polished metal surface on the stage of an Olympus BHSM microscope, which is equipped with $10\times$, $20\times$, and $50\times$ objectives. The power at the sample was 0.1 mW. The spot size of the incident beam was around $1\ \mu\text{m}$ which is greater than the size of the philipsbornite crystal. This means that the spectrum of several crystals was obtained. The microscope is part of a Renishaw 1000 Raman microscope system, which also includes a monochromator, a filter system and a CCD detector (1024 pixels). The Raman spectra were excited by a Spectra-Physics model 127 He–Ne laser producing highly polarised light at 633 nm and collected at a nominal resolution of $2\ \text{cm}^{-1}$ and a precision of $\pm 1\ \text{cm}^{-1}$ in the range between 200 and $4000\ \text{cm}^{-1}$. Repeated acquisitions on the crystals using the highest magnification ($50\times$) were accumulated to improve the signal to noise ratio of the spectra. Because of the lack of signal, over 1200 scans were made. The spectra were collected over night. Raman Spectra were calibrated using the $520.5\ \text{cm}^{-1}$ line of a silicon wafer. The Raman spectrum of at least 10 crystals was collected to ensure the consistency of the spectra.

Infrared spectroscopy

Infrared spectra were obtained using a Nicolet Nexus 870 FTIR spectrometer with a smart endurance single bounce diamond ATR cell. Spectra over the $4000\text{--}525\ \text{cm}^{-1}$ range were obtained by the co-addition of 128 scans with a resolution of $4\ \text{cm}^{-1}$ and a mirror velocity of $0.6329\ \text{cm/s}$. Spectra were co-added to improve the signal to noise ratio. The infrared spectra are given in the supplementary information.

Spectral manipulation such as baseline correction/adjustment and smoothing were performed using the Spectralcalc software package GRAMS (Galactic Industries Corporation, NH, USA). Band component analysis was undertaken using the Jandel 'Peakfit' software package that enabled the type of fitting function to be selected and allows specific parameters to be fixed or varied accordingly. Band fitting was done using a Lorentzian–Gaussian cross-product function with the minimum number of component bands used for the fitting process. The Gaussian–Lorentzian ratio was maintained at values greater than 0.7 and fitting was undertaken until reproducible results were obtained with squared correlations of r^2 greater than 0.995.

Results and discussion

Arsenate vibrations

According to Myneni et al. [37,38] and Nakamoto [39], $(\text{AsO}_4)^{3-}$ is a tetrahedral unit, which exhibits four fundamental vibrations: the Raman active ν_1 symmetric stretching vibration (A_1) at 818 cm^{-1} ; the Raman active doubly degenerate ν_2 symmetric bending vibration (E) observed at 350 cm^{-1} , the infrared and Raman active triply degenerate ν_3 antisymmetric stretching vibration (F_2) found around 786 cm^{-1} , and the infrared and Raman active triply degenerate ν_4 bending vibration (F_2) observed at 405 cm^{-1} . Protonation, metal complexation, and/or adsorption on a mineral surface will cause the change in $(\text{AsO}_4)^{3-}$ symmetry from T_d to lower symmetries, such as C_{3v} , C_{2v} or even C_1 . This loss of degeneracy causes splitting of degenerate vibrations of AsO_4^{3-} and the shifting of the As–OH stretching vibrations to different wavenumbers.

Such chemical interactions reduce AsO_4^{3-} tetrahedral symmetry, as mentioned above, to either C_{3v}/C_3 (corner-sharing), C_{2v}/C_2 (edge-sharing, bidentate binuclear), or C_1/C_s (corner-sharing, edge-sharing, bidentate binuclear, multidentate) [37,38]. In association with AsO_4^{3-} symmetry and coordination changes, the A_1 band may shift to different wavenumbers and the doubly degenerate E and triply degenerate F modes may give rise to several new A_1 , B_1 , and/or E vibrations [37,38]. In the absence of symmetry deviations, $\text{AsO}_3\text{OH}^{2-}$ in C_{3v} symmetry exhibit the ν_s As–OH and ν_{as} and ν_s $\text{AsO}_3\text{OH}^{2-}$ vibrations together with corresponding the δ As–OH in-plane bending vibration, δ As–OH out-of-plane bending vibration, ν_s $\text{AsO}_3\text{OH}^{2-}$ stretching vibration and δ_{as} $(\text{AsO}_3\text{OH})^{2-}$ bending vibration [40–42]. Keller [40] assigned observed the following infrared bands in $\text{Na}_2(\text{AsO}_3\text{OH})\cdot 7\text{H}_2\text{O}$ 450 and 360 cm^{-1} to the δ_{as} (ν_4) $(\text{AsO}_3\text{OH})^{2-}$ bend (E), 580 cm^{-1} to the δ As–OH out-of-plane bend, 715 cm^{-1} to the ν As–OH stretch (A_1), 830 cm^{-1} to the ν_{as} $\text{AsO}_3\text{OH}^{2-}$ stretch (E), and 1165 cm^{-1} to the δ As–OH in-plane bend. In the Raman spectrum of $\text{Na}_2(\text{AsO}_3\text{OH})\cdot 7\text{H}_2\text{O}$, Vansant and Veken [41] attributed observed Raman bands to the following vibrations 55 , 94 , 116 and 155 cm^{-1} to lattice modes, 210 cm^{-1} to $\nu(\text{OH}\cdots\text{O})$ stretch, 315 cm^{-1} to $(\text{AsO}_3\text{OH})^{2-}$ rocking, 338 cm^{-1} to the δ_s $(\text{AsO}_3)^{2-}$ bend, 381 cm^{-1} to the δ_{as} $(\text{AsO}_3\text{OH})^{2-}$ bend, 737 cm^{-1}

to the ν_s As–OH stretch (A_1), 866 cm^{-1} to the ν_{as} $(\text{AsO}_3\text{OH})^{2-}$ stretch (E).

Raman and infrared spectroscopy

The Raman spectrum of philipsbornite in the 100 – 4000 cm^{-1} region is displayed in Fig. 1a and the infrared spectrum in the 500 – 4000 cm^{-1} in Fig. 1b. There are large parts of the spectra where no intensity is observed and therefore the spectra are subdivided into sections so that the peaks may be more readily defined. The Raman spectrum of philipsbornite in the 600 – 1100 cm^{-1} region is shown in Fig. 2a and the infrared spectrum in the 500 – 1300 cm^{-1} region in Fig. 2b. The Raman spectrum displays an asymmetric peak at 831 cm^{-1} with a shoulder on the high wavenumber side. Component bands may be resolved as is shown. These peaks are attributed to the ν_1 $(\text{AsO}_4)^{3-}$ symmetric stretching vibration (A_1). It is apparent that the band due to the ν_3 $(\text{AsO}_4)^{3-}$ antisymmetric stretching vibration is not observed as a separate band but is coincident with the symmetric stretching vibration. The Raman spectrum of philipsbornite is reported in the RRUFF data base (<http://rruff.info/Philipsbornite>), however, no interpretation is given. In this spectrum a broad Raman band at around 850 cm^{-1} is observed. The width of the peak suggests that is composed of a series of underlying bands. In the infrared spectrum, these bands are observed as overlapping bands. Two bands at 762 and 814 cm^{-1} are attributed to the ν_3 $(\text{AsO}_4)^{3-}$ antisymmetric stretching vibrations. The lower intensity infrared peak at 850 cm^{-1} may be due to the ν_1 $(\text{AsO}_4)^{3-}$ symmetric stretching vibration. In our Raman spectrum no bands in the 1000 – 1200 cm^{-1} region was observed; yet a considerable number of bands are observed in the infrared spectrum. Infrared bands are observed at 1005 , 1048 , 1086 , 1113 , 1187 and 1272 cm^{-1} . These bands are attributed to sulphate or phosphate in the mineral. In the spectrum in the RRUFF data base two Raman peaks are found at 980 and 1020 cm^{-1} . These bands may be assigned to phosphate bands.

The Raman spectrum of philipsbornite in the 100 – 600 cm^{-1} region is reported in Fig. 3. Raman bands are observed at 325 , 336 , 347 , 357 , 376 and 399 cm^{-1} . The first four bands are assigned to the ν_2 $(\text{AsO}_4)^{3-}$ symmetric bending vibration (E) and the latter

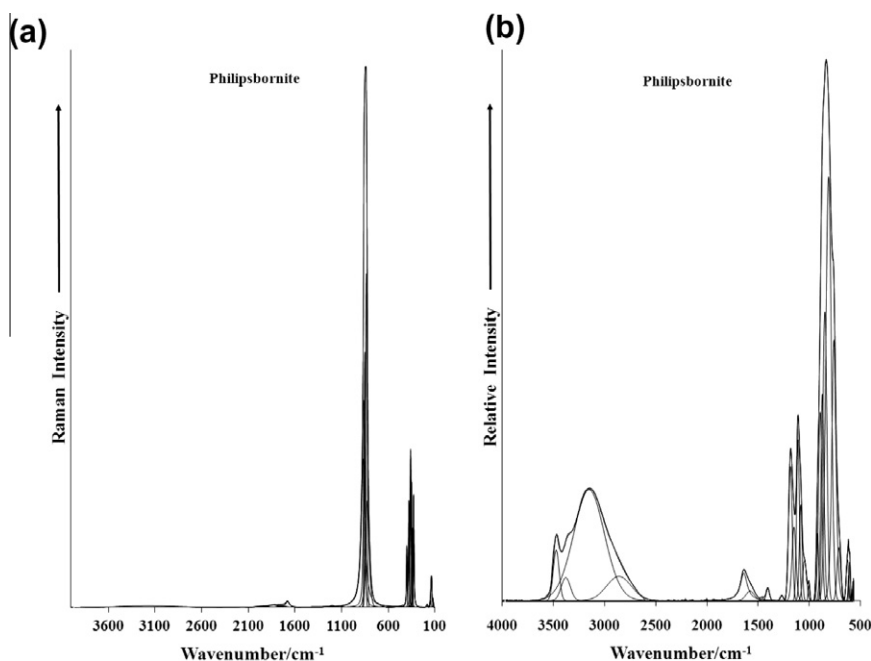


Fig. 1. (a) Raman spectrum of philipsbornite over the 100 – 4000 cm^{-1} range and (b) infrared spectrum of philipsbornite over the 500 – 4000 cm^{-1} range.

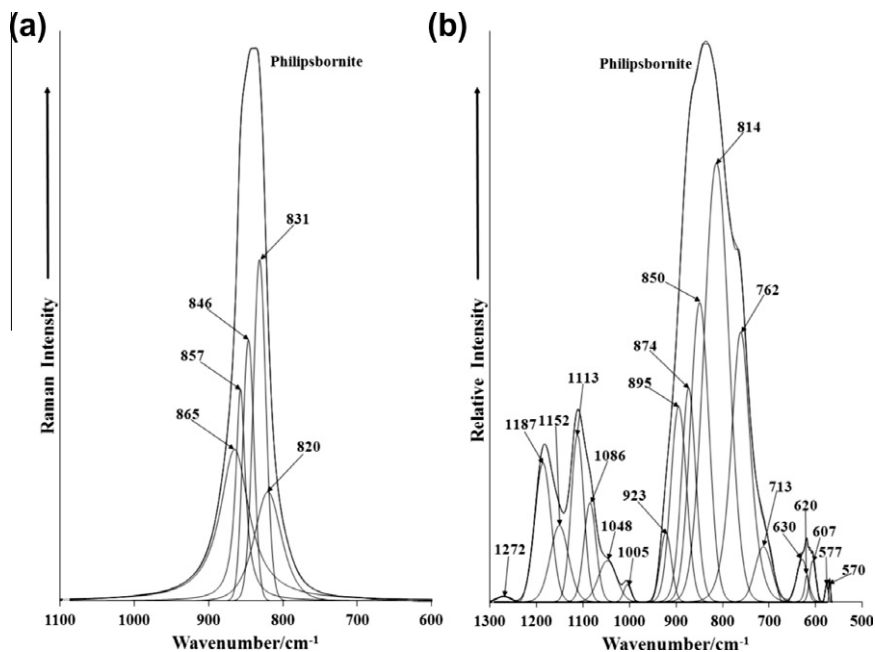


Fig. 2. (a) Raman spectrum of philipsbornite over the 600–1100 cm^{-1} range and (b) infrared spectrum of philipsbornite over the 500–1300 cm^{-1} range.

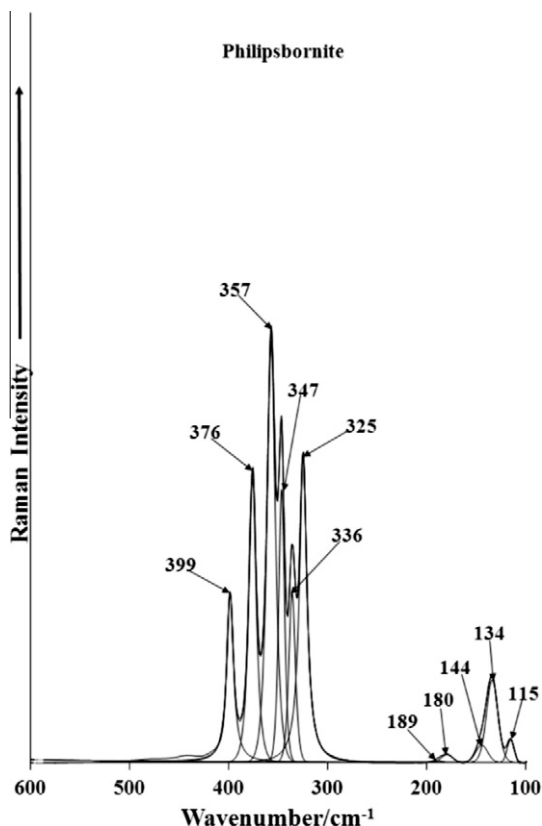


Fig. 3. Raman spectrum of philipsbornite over the 100–600 cm^{-1} region.

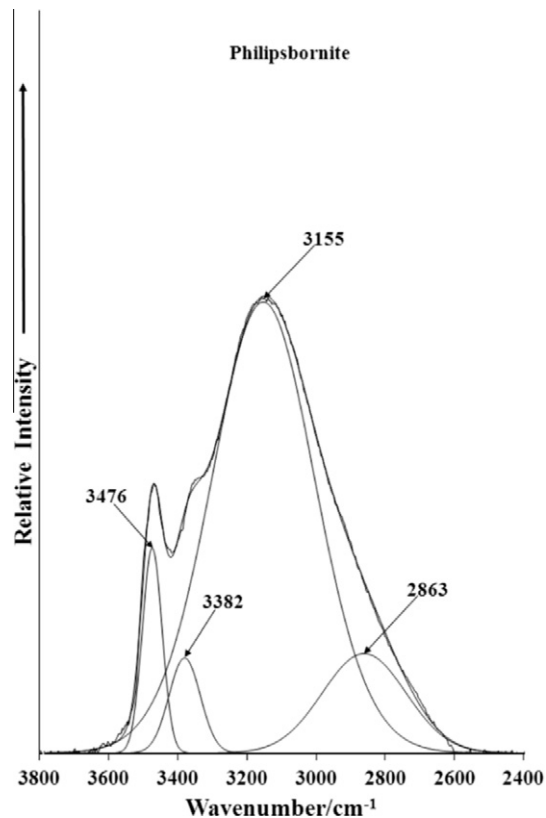


Fig. 4. Infrared spectrum of philipsbornite over the 2400–3800 cm^{-1} range.

two bands are assigned to the ν_4 bending vibration (F_2). The assignment of these bands is in harmony with the analysis of arsenate vibrations according to Myneni et al. [37,38] and Nakamoto [39]. The observation of multiple bands suggests that the degeneracy of the bending modes has been removed. The doubly degenerate E and triply degenerate F modes give rise to several new A_1 , B_1 ,

and/or E vibrations as is observed in the spectrum shown in Fig. 3 [37,38]. A series of bands at 115, 134, 144, 180 and 189 cm^{-1} are simply described as external vibrations often referred to as lattice vibrations.

The infrared spectrum of philipsbornite in the hydroxyl stretching region is reported in Fig. 4. The Raman spectrum shows a very low intensity band centred upon 3162 cm^{-1} . The infrared spectrum

shows greater intensity with infrared bands observed at 2863, 3155, 3382 and 3476 cm^{-1} . This latter band is assigned to the OH stretching vibrations of the OH units in the philipsbornite structure $(\text{PbAl}_3(\text{AsO}_4)_2(\text{OH})_5 \cdot \text{H}_2\text{O})$. The infrared bands at 3155 and 3382 cm^{-1} are assigned to water stretching vibrations.

Studies have shown a strong correlation between OH stretching frequencies and both O···O bond distances and H···O hydrogen bond distances [43–46]. Libowitzky showed that a regression function can be employed relating the hydroxyl stretching frequencies with regression coefficients better than 0.96 using infrared spectroscopy [47]. The function is described as: $\nu_1 = (3592 - 304) \times 109^{\frac{-d(\text{O}-\text{O})}{0.1321}} \text{cm}^{-1}$. Thus OH–O hydrogen bond distances may be calculated using the Libowitzky empirical function. The Raman spectrum of philipsbornite is not suitable for the calculations of hydrogen bond distances. Hydrogen bond distances for philipsbornite of 2.8648 Å (3476 cm^{-1}), 2.7864 Å (3382 cm^{-1}), 2.6896 Å (3155 cm^{-1}) and 2.6220 (2863 cm^{-1}) are calculated.

A range of hydrogen bond distances are observed from reasonably strong to weak hydrogen bonding. This range of hydrogen bonding contributes to the stability of the mineral. Two types of OH units can be identified in the structures of philipsbornite. The infrared spectrum of philipsbornite may be divided into two groups of OH stretching wavenumbers; namely 3300–3500 cm^{-1} and 2800–3200 cm^{-1} . This distinction suggests that the strength of the hydrogen bonds as measured by the hydrogen bond distances can also be divided into two groups according to the H-bond distances. An arbitrary cut-off point may be 2.74 Å based upon the wavenumber 3300 cm^{-1} . The first two hydrogen bond distances are thus defined as weak hydrogen bonds and the latter two as stronger hydrogen bonds.

Conclusions

Raman spectroscopy has proved most useful for the study of the mineral philipsbornite, a member of the crandallite mineral group. Such a mineral contains arsenate and the formation of the mineral offers a mechanism for the accumulation of arsenate. Raman spectroscopy of philipsbornite shows a broad spectral profile centred upon around 840 cm^{-1} . This profile may be deconvoluted into component bands. It is apparent that the profile contains bands due to both the symmetric stretching and antisymmetric stretching modes. Raman bands observed at 325, 336, 347, 357, 376 and 399 cm^{-1} are assigned to the $\nu_2(\text{AsO}_4)^{3-}$ symmetric bending vibration (E) and to the ν_4 bending vibration (F_2). The observation of multiple bending modes supports the concept of a reduction in symmetry of the arsenate anion. Raman spectroscopy shows that the philipsbornite is very pure with only the arsenate anion being present. This is unusual as minerals of the crandallite form solid solutions very readily. It would be expected to see the presence of phosphate or even sulphate in the mineral.

Minerals of the crandallite group lend themselves to analysis by Raman spectroscopy. Individual crystals may be selected for Raman spectroscopic analysis. The spatial resolution is around 1 μm , compared with infrared spectroscopy where the spatial resolution is at best 30 μm . This means that the correct crystal can be selected for analysis. Infrared spectroscopy often measures mixtures of minerals because of this lack of spatial resolution. This is exemplified by the analysis of philipsbornite as detailed in this manuscript. Raman spectroscopy proves that the philipsbornite is a pure arsenate mineral. Some removal of the degeneracy of the vibrational modes is observed. In comparison infrared spectroscopy shows the philipsbornite contains anions other than the

arsenate anion. Of course, this is not correct. This simply confirms Raman spectroscopy as a very powerful technique for the characterisation of the molecular structure of philipsbornite.

Acknowledgments

The financial and infra-structure support of the Queensland University of Technology, Chemistry discipline is gratefully acknowledged. The Australian Research Council (ARC) is thanked for funding the instrumentation. The Australian Museum is thanked for the loan of the mineral philipsbornite.

References

- [1] K. Walenta, M. Zwiener, P.J. Dunn, Neues Jahrb. Min. (1982) 1–5.
- [2] R.G. Schwab, C. Goetz, H. Herold, N. Pinto de Oliveira, Neues Jahrb. Min. (1991) 97–112.
- [3] R.G. Schwab, H. Herold, C. Goetz, N. Pinto de Oliveira, Neues Jahrb. Min. (1990) 113–126.
- [4] J. Sejkora, J. Cejka, V. Srein, M. Novotna, J. Ederova, Neues Jahrb. Min. (1998) 145–163.
- [5] J. David, J. Jansa, F. Novak, I. Prachar, Vestnik Ustred. Ust. Geol. 65 (1990) 367–369.
- [6] P. Keller, W. Bartelke, Min. Rec. 13 (1982) 137–147.
- [7] S. Matsubara, A. Kato, T. Kamiya, Chigaku Ken. 39 (1990) 101–105.
- [8] K. Schmetzer, G. Tremmel, O. Medenbach, Neues Jahrb. Min. (1982) 248–254.
- [9] R.S. Bottrill, P.A. Williams, S. Dohnt, S. Sorrell, N.R. Kemp, Aust. J. Min. 12 (2006) 59–90.
- [10] K. Norrish, Trans., Int. Congr. Soil Sci., 9th, 2 (1968) 713–723.
- [11] M.C.F. Magalhaes, M.C.M. Silva, Neues Jahrb. Min. 134 (2003) 735–743.
- [12] R.L. Frost, E.C. Keeffe, S. Bahfenne, Spectrochim. Acta A75 (2010) 1476–1479.
- [13] R.L. Frost, B.J. Reddy, E.C. Keeffe, Spectrochim. Acta A77 (2010) 388–396.
- [14] R.L. Frost, Spectrochim. Acta A71 (2009) 1788–1794.
- [15] R.L. Frost, Spectrochim. Acta A72 (2009) 903–906.
- [16] R.L. Frost, S. Bahfenne, J. Graham, Spectrochim. Acta A71 (2009) 1610–1616.
- [17] R.L. Frost, J. Cejka, Spectrochim. Acta A71 (2009) 1959–1963.
- [18] R.L. Frost, J. Cejka, M.J. Dickfos, Spectrochim. Acta A71 (2009) 1799–1803.
- [19] R.L. Frost, B.J. Reddy, S. Bahfenne, J. Graham, Spectrochim. Acta A72 (2009) 597–604.
- [20] R.L. Frost, J. Cejka, J. Sejkora, J. Plasil, B.J. Reddy, E.C. Keeffe, Spectrochim. Acta A78 (2011) 494–496.
- [21] R.L. Frost, S.J. Palmer, Spectrochim. Acta A78 (2011) 248–252.
- [22] R.L. Frost, S.J. Palmer, Spectrochim. Acta A78 (2011) 1255–1260.
- [23] R.L. Frost, S.J. Palmer, Spectrochim. Acta A78 (2011) 1250–1254.
- [24] R.L. Frost, S.J. Palmer, Spectrochim. Acta A79 (2011) 1794–1797.
- [25] R.L. Frost, S.J. Palmer, Spectrochim. Acta A79 (2011) 1215–1219.
- [26] R.L. Frost, S.J. Palmer, A vibrational spectroscopic study of the mixed anion mineral sanjuanite $\text{Al}_2(\text{PO}_4)(\text{SO}_4)(\text{OH}) \cdot 9\text{H}_2\text{O}$, Spectrochim. Acta, Part A 79 (2011) 1210–1214.
- [27] R.L. Frost, S.J. Palmer, S. Bahfenne, Spectrochim. Acta A78 (2011) 1302–1304.
- [28] R.L. Frost, S.J. Palmer, R.E. Pogson, Spectrochim. Acta A79 (2011) 1149–1153.
- [29] R.L. Frost, B.J. Reddy, S.J. Palmer, E.C. Keeffe, Spectrochim. Acta A78 (2011) 996–1003.
- [30] M. Filippi, V. Machovic, P. Drahota, V. Bohmova, Appl. Spectrosc. 63 (2009) 621–626.
- [31] S.V. Gevorkyan, A.A. Petrunina, A.S. Povarennykh, Konstit. Svoistva Min. 10 (1976) 51–59.
- [32] R.L. Frost, M.L. Weier, W. Martens, S. Mills, J. Mol. Struct. 752 (2005) 178–185.
- [33] R.L. Frost, S. Bahfenne, J. Cejka, J. Sejkora, J. Plasil, S.J. Palmer, E.C. Keeffe, I. Nemeč, J. Raman Spectrosc. 42 (2011) 56–61.
- [34] R.L. Frost, Y. Xi, R.E. Pogson, Spectrochim. Acta A91 (2012) 301–306.
- [35] J. Haupt, Min. Rec. 19 (1988) 381–388.
- [36] A.V. Brown, N.J. Page, A.H. Love, Can. Min. 26 (1988) 161–175.
- [37] S.C.B. Myneni, S.J. Traina, G.A. Waychunas, T.J. Logan, Geochim. Cosmochim. Acta 62 (1998) 3285–3300.
- [38] S.C.B. Myneni, S.J. Traina, G.A. Waychunas, T.J. Logan, Geochim. Cosmochim. Acta 62 (1998) 3499–3514.
- [39] K. Nakamoto, Infrared and Raman Spectra of Inorganic and Coordination Compounds, Wiley, New York, 1986.
- [40] P. Keller, Neues Jb. Miner. Mh. (1971) 491–510.
- [41] F.K. Vansant, B.J.V.D. Veken, J. Mol. Struct. 15 (1973) 439–444.
- [42] F.K. Vansant, B.J.V.D. Veken, H.O. Desseyn, J. Mol. Struct. (1973) 425–437.
- [43] J. Emsley, Very strong hydrogen bonding, Chem. Soc. Rev. 9 (1980) 91–124.
- [44] H. Lutz, Struct. Bonding 82 (1995) 85–103.
- [45] W. Mikenda, J. Mol. Struct. 147 (1986) 1–15.
- [46] A. Novak, Struct. Bonding 18 (1974) 177–216.
- [47] E. Libowitzky, Monat. Chem. 130 (1999) 1047–1049.